Upper critical field H_{c2} calculations for the high critical temperature superconductors considering inhomogeneities

E. S. Caixeiro, J. L. González, and E. V. L. de Mello
Departamento de Física, Universidade Federal Fluminense, Niterói, RJ 24210-340, Brazil
(Received 26 March 2003; revised manuscript received 19 September 2003; published 29 January 2004)

We perform calculations to obtain the H_{c2} curve of high temperature superconductors (HTSCs). We consider explicitly the fact that HTSCs possess intrinsic inhomogeneities by taking into account a nonuniform charge density $\rho(r)$. The transition to a coherent superconducting phase at a critical temperature T_c corresponds to a percolation threshold among different superconducting regions, each one characterized by a given $T_c(\rho(r))$. Within this model we calculate the upper critical field H_{c2} by means of an average linearized Ginzburg-Landau equation modified to take into account the distribution of local superconducting temperatures $T_c[\rho(r)]$. This approach explains some of the anomalies associated with H_{c2} and why several properties like the Meissner and Nernst effects are detected at temperatures much higher than T_c.

DOI: 10.1103/PhysRevB.69.024521 PACS number(s): 74.72.−h, 74.20.−z, 74.81.−g

I. INTRODUCTION

High critical temperature superconductors (HTSCs) were discovered 15 years ago,[1] but many of their properties remains not well explained. Some of their features are completely different from the low temperature superconductors, for example, the H-T phase diagram of the HTSC possesses, in certain cases, a positive curvature for $H_{c2}(T)$, with no evidence of saturation at low temperatures.[2–4] This lack of saturation at low temperatures may minimize the importance of strong fluctuations of the order parameter which was one of the earlier leading ideas.[5,6] Furthermore, this behavior cannot be explained by the classical WHH (Werthamer-Helfand-Hohenberg) theory for superconductors[7,8] where $H_{c2}(T)$ exhibits a negative curvature and saturates at low temperatures.

In order to interpret this unusual behavior and furnishes ground to the H_{c2} positive curvature many different possibilities were proposed such as, for instance, the interplay between Anderson localization and superconductivity which affects the coherent length near the mobility edge,[9] the effect of correlations among magnetic impurities which leads to a weakening of the pair breaking process,[10] mesoscopic fluctuations,[11] the depletion of vortex viscosity or local pairs confined to small superconducting regions coupled through a normal host due to anisotropic quasiparticle relaxation rate around the Fermi surface,[12] the effective two component (boson-fermion) model,[13] Luttinger liquid behavior in the normal state,[14,15] bipolaron superconductivity,[16] charge-density waves, and stripes.[17]

On the other hand, another feature that has recently received considerable attention is the intrinsic inhomogeneous distribution of charge (or doping level) and superconducting gaps, as demonstrated by the scanning tunneling microscopy (STM)/S experiments.[18–20] Based on these measurements and on a number of others, like neutron diffraction,[21–24] we have proposed a general theory to explain the main features of the HTSC phase diagram.[25,26] The main point is that near the pseudogap temperature T^* (Ref. 27) some localized regions become superconducting, and the size of these regions increases as the temperature is lowered and, at the critical temperature T_c, these superconducting regions percolate, and the system becomes able to hold a dissipationless current. This scenario is consistent with the Meissner effect above T_c measured by Iguchi *et al.*[28] and the diamagnetic signal above T_c which has also been measured by other groups by susceptibility.[29] The drift of magnetic vortices expected to occur in the a superconductor phase has also been measured in HTSCs at temperatures above T_c through the Nernst effect.[30]

In this paper we develop a unified view of all these anomalous properties to explain the observed features of the upper critical field H_{c2} unusual properties in HTSCs. In our approach the pseudogap temperature T^* is where small static superconducting regions start to develop.[26] The intrinsic inhomogeneities in the charge produce superconducting gaps which vary locally inside a given sample and, as the temperature decreases below T^*, the superconducting regions start to grow, as demonstrated by Meissner effect measurements.[28] At temperatures below T^*, but above the critical temperature T_c, there is no long range order but there are several isolated local superconducting regions inside the sample. This scenario explains why there is some indications that H_{c2} does not vanish at T_c (Ref. 31) but at a much larger value; also a much larger magnetization than that expected, above T_c, was recently measured.[29] The main difficulty to perform calculations in this scenario is the lack of information on the inhomogeneous distribution of charge in a given sample. Based on the experimental results which led to the idea of stripes[32,33] and on the STM/S results, we have proposed a bimodal distribution for the charge inside a given HTSC.[26] Although we do not know the exact form of such distribution, it mimics the antiferromagnetic (AF) insulator regions (insulator branch) and the metallic regions (metallic branch) and contains several features found in the cuprates. Here we will apply such a distribution, derived in Ref. 26, to calculate the contribution of resulting superconducting regions to estimate the magnetic response for some materials and compare with the experimental results. This is accomplished through a simple model to compute the contribution

of the superconducting regions to the upper critical field H_{c2}, considering that each of these regions acts as an independent superconducting region whose H_{c2} is described by the Ginzburg-Landau (GL) equation. All the contributions from different regions are computed to give the total upper critical field of a given superconducting compound. This is a clear phenomenological approach that, according to the GL theory, yield good results near the critical temperatures.

It is worthwhile to mention that Ref. 12 also inferred that the positive curvature of H_{c2} could be due to pair formation in small grains with local T_c higher than the bulk T_c. Therefore, we can see that several attempts had been published[10–13] connecting H_{c2} and its features with the effects of some type of disorder. By the same token, below we apply our recently developed theory[26] on the inhomogeneities of cuprates and pseudogap phenomenon to evaluate a theory for the H_{c2} of these materials.

This paper is divided as follows: In Sec. II we present the density of charge distribution and the phase diagram of a selected compound of the LSCO family. In Sec. III the upper critical field H_{c2} from the GL theory is considered and generalized with the inclusion of the inhomogeneous superconducting regions. In Sec. IV we compare the theoretical results with some selected experimental data of the LSCO family and optimum Bi2212 high T_c. A good qualitative agreement is observed. In Sec. V we make the final analyses and conclusions.

II. DENSITY OF CHARGE DISTRIBUTION

Just for completeness, we will briefly outline the basic ideas concerned with the inhomogeneous charge distribution introduced in Ref. 26. To model this inhomogeneous medium we consider a phenomenological distribution of probability $P[\rho(r)]$ of a given local charge density $\rho(r)$. The differences in the local charge densities yield insulator and metallic regions. For simplicity we hereafter make $\rho(r)=\rho$.

The distribution $P[\rho(r)]$ we consider is a combination of a Gaussian and a Poisson distribution, which becomes the appropriate distribution to deal with the high and low density compounds,[26] that is, the whole phase diagram. The main features of $P(\rho)$ is that it has two branches: an insulating one with $0 \leqslant \rho \leqslant 0.05$, and a metallic one which starts at ρ_m.

For most compounds $\rho_m \approx \langle\rho\rangle$, where $\langle\rho\rangle$ is the average density of a compound. In Fig. 1 we show the phase diagram for the LSCO $\langle\rho\rangle=0.15$ compound together with the charge distribution and experimental data of Refs. 34 and 35. Since the local critical temperature $T_c(\rho)$ is a decreasing function of ρ, the maximum T_c is $T_c(\langle\rho\rangle)$, which is therefore the system pseudogap temperature T^*. Upon cooling below T^* part of the metallic regions become superconducting. At $T=T_c$ 59% of the material is in the superconducting phase and we say that the superconducting regions percolate.[26] As the temperature decreases even further the percentage of material in the superconducting phase increases.

In order to study the effect of the charge distribution on our results we have considered a constant distribution and a linear decreasing distribution, with metallic and insulating branches, evaluated with the densities ρ_c and ρ_p (see Fig. 1)

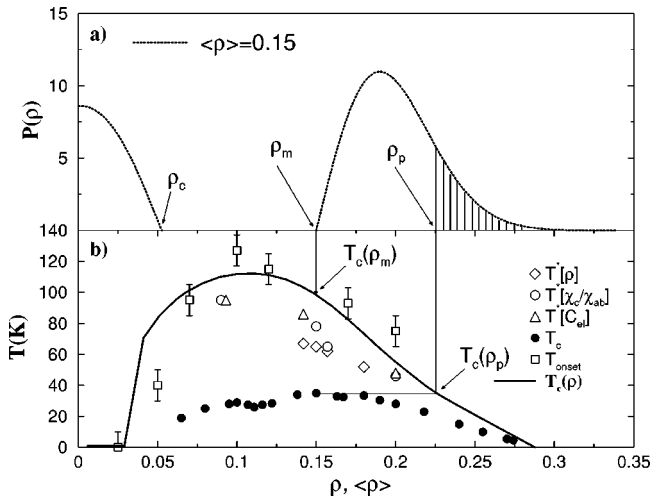

FIG. 1. (a) The distribution $P(\rho)$ for the LSCO $\langle\rho\rangle=0.15$ compound is shown. The arrows indicates the density $\rho_c=0.05$, the percolation density $\rho_p=0.225$, and ρ_m, with $\rho_m=\langle\rho\rangle$. The hachured part indicates the region above the percolation threshold ρ_p, i.e., the region below the superconducting critical temperature T_c. The percolate threshold is reached when 59% of the material is in the superconducting state. (b) The theoretical local superconducting critical temperatures $T_c(\rho)$ for this compound is shown as the solid line, together with the experimental pseudogap temperatures T^* of Refs. 34 and 35. The filled black circles are the experimental critical temperatures T_c of the LSCO family from Ref. 35. The vertical and horizontal lines indicates $T_c(\rho_p)=T_c$.

for $\rho_m=0.15$, and in the same range of densities. The results are shown in Fig. 2(a) in Sec. IV and indicate that the qualitative behavior remains the same, i.e., the inhomogeneities seem to be the cause of the positive curvature, but the quantitative agreement is worst than the results from the distribution derived by the STM experiments and used in our calculations.

III. CALCULATIONS

It is well known that most HTSCs are type-II superconductors.[36] For these types of superconductors there are two critical fields in the H-T phase diagram: the lower H_{c1} and the upper H_{c2}. Above H_{c2} the material returns to the normal metal state. By definition, one expects the superconductivity to disappear above the upper critical field H_{c2}.

In the case of an external magnetic field parallel to the c direction, i.e., perpendicular to the CuO_2 planes (ab direction), the GL upper critical field is given by[37–39]

$$H_{c2}(T)=\frac{\Phi_0}{2\pi\xi_{ab}^2(T)}, \tag{1}$$

where $\Phi_0=hc/2e$ is the flux quantum and $\xi_{ab}(T)$ is the GL temperature dependent coherence length in the ab plane.[6,37,40] Therefore, H_{c2} is determined by the coherence length $\xi_{ab}(T)$ of the superconductor, which is treated as a phenomenological parameter. In terms of the GL parameters the coherence length is given by

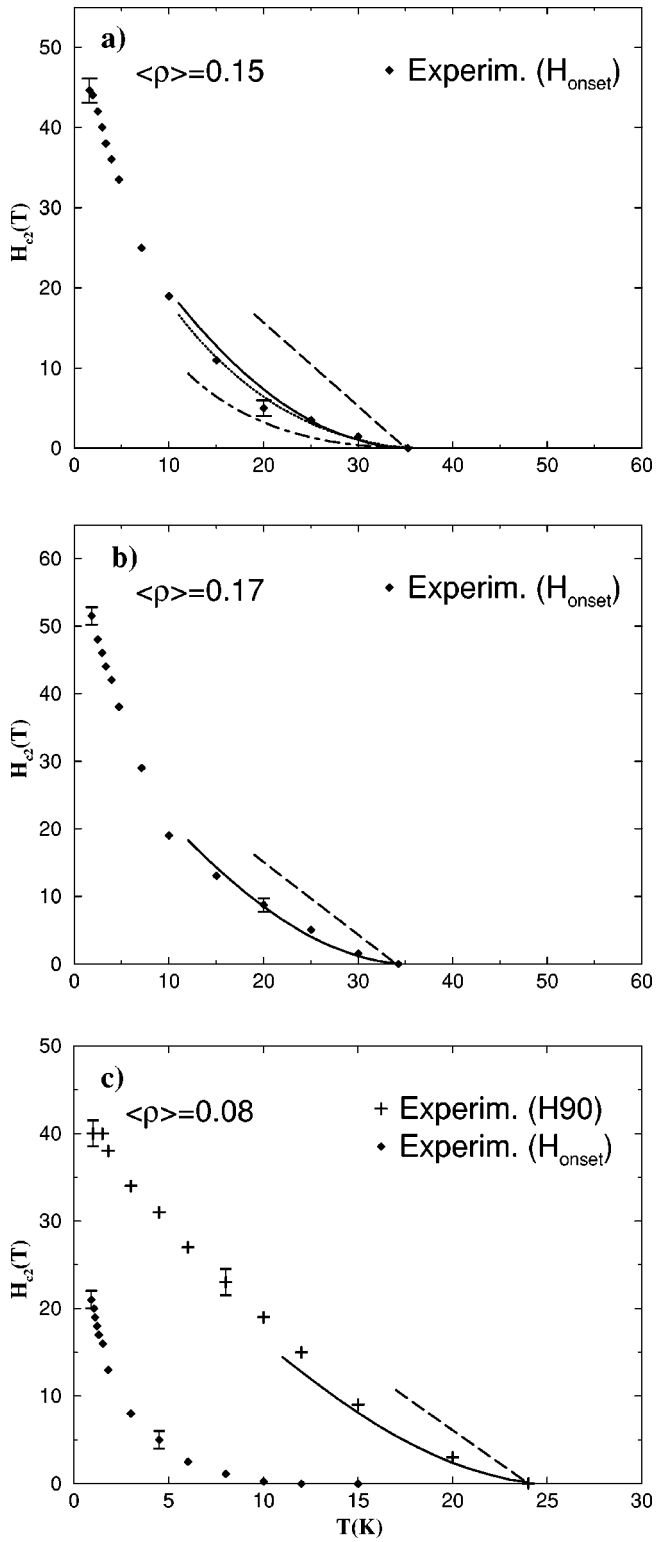

FIG. 2. Theoretical results of $H_{c2}(T)$ (solid lines) of the LSCO series considering the distribution of Ref. 26 together with the experimental data of Ref. 2. The dashed line is a pure GL fitting of Eq. (3). In (a) the results for a constant distribution (dot-dashed line) and a linear distribution (dotted line) are also shown.

$$\xi_{ab}^2(T)=\frac{\hbar^2}{2m_{ab}\alpha(T)}=\xi_{ab}^2(0)\left(\frac{T_c}{T_c-T}\right) \quad (T<T_c), \quad (2)$$

where $\xi_{ab}^2(0)=\hbar^2/2m_{ab}aT_c$ is the extrapolated coherence length, m_{ab} is the part of the mass tensor for the *ab* plane, and a is a constant.[39] Using the BCS formula $\xi\sim v_F/k_BT_c$ we expect a shorter coherence length for HTSCs relative to the low temperature superconductors due to their ten times higher T_c's. However, due to the lower density of carriers,[39] v_F in these materials is also small, which results in a very short coherence length, $\xi\sim 10$ Å. A typical value for the extrapolated coherence length which we use in our calculations is $\xi_{ab}(0)\sim 15$ Å and $\xi_c(0)\sim 4$ Å for the YBCO (Ref. 39) and $\xi_{ab}(0)\sim 32$ Å and $\xi_c(0)\sim 7$ Å for LSCO,[39,41] where $\xi_c(0)$ is the coherence length in the *c* direction. One should note that $\xi_c(0)$ is smaller than $\xi_{ab}(0)$ and is of the order of the spacing between adjacent conducting CuO_2 planes.

Therefore, the GL upper critical field may be written as

$$H_{c2}(T)=\frac{\Phi_0}{2\pi\xi_{ab}^2(0)}\left(\frac{T_c-T}{T_c}\right) \quad (T<T_c). \quad (3)$$

Let us now apply this expression to a HTSC with intrinsic inhomogeneities in the charge distribution.

When considering the inhomogeneity of the HTSC at temperatures below T^*, isolated superconducting regions may exist in the form of separated islands even in magnetic fields $H>H_{c2}(T)$.[42,43] For temperatures above T_c there is no long range order but, due to the various different local values of $T_c[\rho(r)]$ superconducting regions may exist in the form of separated regions. Here we calculate the upper critical field H_{c2} for a given sample assuming that each isolated or connected superconducting region displays a local H_{c2}^i which is given by the linearized GL equation with an effective mass tensor.[37,44] Since a given local superconducting region "i" has a local temperature $T_c(i)$ with a probability P_i and a local coherence length ξ_i, it will contribute to the upper critical field with a local linear upper critical field $H_{c2}^i(T)$ near $T_c(i)$. Therefore, the total contribution of the local superconducting regions to the upper critical field is the sum of all the $H_{c2}^i(T)$'s. Thus, applying Eq. (3), the H_{c2} for an entire sample is

$$H_{c2}(T)=\frac{\Phi_0}{2\pi\xi_{ab}^2(0)}\frac{1}{W}\sum_{i=1}^{N}P_i\left(\frac{T_c(i)-T}{T_c(i)}\right)$$

$$=\frac{1}{W}\sum_{i=1}^{N}P_iH_{c2}^i(T) \quad (T<T_c(i)\leqslant T_c), \quad (4)$$

where N is the number of superconducting regions, or superconducting islands each with its local $T_c(i)\leqslant T_c$ and $W=\Sigma_{i=1}^{N}P_i$ is the sum of all the P_i's. As we already mentioned, at temperatures above T_c there are isolated superconducting regions, while below T_c these regions percolate and the system may hold a dissipationless current. Since H_{c2} is experimentally measured at $T<T_c(H=0)$, it is the field which destroys the superconducting clusters with $T<T_c(i)\leqslant T_c$, leading the system below the percolation threshold, that is, less than 59% of the system is in the superconducting state. The first regions which are broken are the weakest ones, which have critical temperatures $T_c(i)$'s lower than

$T_c(H=0)$. The mechanism is the following: at a temperature $T<T_c$ most of the system is superconducting and a small applied field first destroys the superconducting regions with lower $T_c(i)$'s, without loss of long range order. Increasing the applied field causes more regions to become normal and, eventually, when the regions with $T_c(i)\approx T_c$ turn to the normal phase, the system is about to have a nonvanishing resistivity. This value of the applied field is taken as the H_{c2} in our theory, and it is the physical meaning of Eq. (4). Thus, at a given temperature T, we sum the superconducting regions with $T<T_c(i)\leqslant T_c$, with their respective probabilities.

It is important to notice that the STM experiments have demonstrated that the size of a region with constant superconducting gap is of the order of 20 Å.[18–20] These results have also been obtained by μSR experiments.[45] According to the discussion in Sec. I, at T^* some small superconducting isolated islands (or droplets) start to appear through the system. Therefore, near T^* the GL approach should not be valid because the size of an island coherence length with $T_c(i)\approx T^*$ is of the same order of the superconducting islands. As the temperature decreases the superconducting islands start to unite forming larger inhomogeneous superconducting regions. At T_c they percolate, occupying about 59% of the system. At $T<T_c$ the occupied superconducting volume is comparable to the size of the system and clearly much larger than the typical coherence length ξ_i of the different inhomogeneous regions. Consequently, we may use the GL theory to calculate the upper critical field of these different superconducting regions which form the whole condensate, and the total sample H_{c2} is the sum of these individual inhomogeneous contributions as in Eq. (4).

IV. COMPARISON WITH EXPERIMENTAL DATA

In this section we compare the results of Eq. (4) with the experimental upper critical field data of Refs. 2 and 31 of the LSCO family and near optimum Bi2212.

The experimental upper critical field H_{c2} of the HTSC may be obtained from the resistivity measurements as it is the field relative to a fraction of the ''normal-state'' resistivity.[2,39] The correct fraction which leads to the upper critical field is still controversial, and there is no conclusion as to whether H_{c2} may correspond to the beginning, the middle, or the top (end) of the resistivity curves.[2,3] Another way to obtain H_{c2} is from the field dependence of the transport line entropy derived from the Nernst signal.[31] Despite this difficulty we attempt here to compare the theoretical results with the available experimental data. For this purpose we identified some applied magnetic fields of Ref. 2 and H^* of Ref. 31 as the upper critical fields for the selected compounds studied due to the reasons below.

By definition, H_{onset} from the resistive measurements of Ref. 2 is defined as the magnetic field at which the resistivity ρ first is detected to deviate from the zero in the ρ vs H curves, and this is the assumption used in Eq. (4) and, therefore, is our definition of $H_{c2}(T)$. Furthermore, it is reasonable to take T_c from the H-T phase diagram as the temperatures where $H_{onset}=0$. However, it is experimentally observed[2] that for some compounds H_{onset} vanishes at temperatures much smaller than the known values of T_c. This is because the superconducting transition is sharp at low fields, but spreads itself over a large interval of temperatures as the field increases. As a consequence one defines the field Hx, x being a percentage of the normal state resistivity. In some cases the difference between H_{onset} and $H90$ (90% of the normal-state resistivity) may be about 50% of T_c.[2] When this is the case the correct H_{c2} may be between these two fields. In our calculations from Eq. (4) H_{c2} is calculated for $T\leqslant T_c$ and always vanishes at T_c, with H_{c2} being in principle the H_{onset} field. By the same token, for the Nernst signal measurements of Ref. 31, H^* may be considered the upper critical field since it represents an intrinsic field which controls the onset of the flux-flow dissipation and vanishes at a temperature close to T_c. Therefore, H^* may be compared with H_{onset}. In agreement with Wang *et al.*,[31] attempts to find H_{c2} using the resistivity invariably turn up a curve akin to H^*.

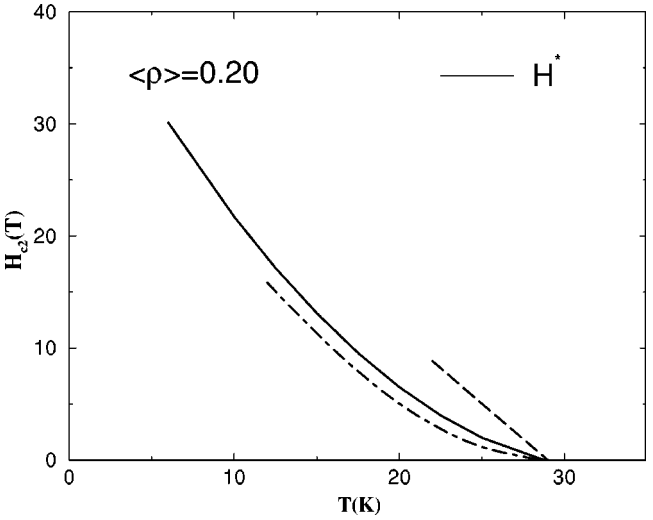

FIG. 3. Theoretical results of $H_{c2}(T)$ (dot-dashed line) for the $\langle\rho\rangle=0.20$ of the LSCO series together with the Nernst signal measurements curve of Ref. 31 (solid line). The dashed line is a GL fitting.

Now, in order to compare with the experimental fields of Ref. 2, we plot $H_{c2}(T)$ with the measured H_{onset} for the cases of $\langle\rho\rangle=0.15$ [Fig. 2(a)] and $\langle\rho\rangle=0.17$ [Fig. 2(b)] of the LSCO series. Also in Fig. 2(a), we plot the results of constant and linear charge distributions together with the bimodal distribution of Ref. 26. As one can see, the distributions yield very similar results, which shows that the calculations do not depend on the details of the charge distribution, although without a distribution of $T_c(i)$'s we simply obtain a GL linear behavior.

For the case of $\langle\rho\rangle=0.08$ [Fig. 2(c)] we compared our results with $H90$ since this field vanishes at $T_c\approx 24$ K, which is the value of T_c obtained from the phase diagram of Ref. 26, while H_{onset} vanishes at $T\approx 12$ K. In Fig. 3 one can see the results for $\langle\rho\rangle=0.20$ compared with H^* from the Nernst-signal measurements of Ref. 31. For the near-optimum Bi2212 we compared our results with $H50$ (Fig. 4) of Ref. 2, which vanishes at $T_c\approx 80$ K and is in accordance

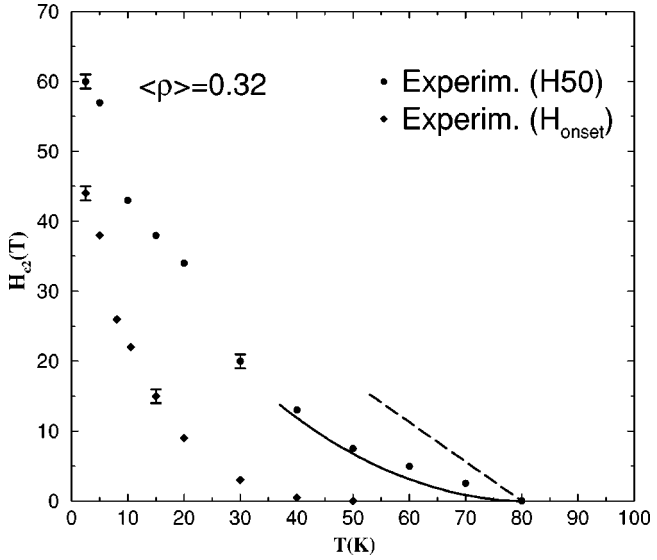

FIG. 4. Theoretical results of $H_{c2}(T)$ (solid line) of the near optimum Bi2212 together with the experimental points of Ref. 2. A pure GL fitting using Eq. (3) is also shown (dashed line) for comparison.

with the phase diagram of Ref. 26, while H_{onset} vanishes at $T \approx 50$ K. Also, in Figs. 2(c) and 4 the experimental points of H_{onset} are shown for comparison. For the LSCO series a coherence length of $\xi_{ab}(0) = 30$ Å was adopted, which is in accordance with the measurements of Refs. 39, 41, and 46. This value of $\xi_{ab}(0)$ leads to $H_{c2}(0) = \Phi/2\pi\xi_{ab}^2(0) = 32$ T. For the Bi2212 a coherence length of $\xi_{ab}(0) = 27$ Å was considered, which is in accordance with Ref. 46. Similarly one gets $H_{c2}(0) = 45$ T. These discrepancies for the low temperature values of $H_{c2}(T)$ is clearly due to the GL expressions [Eqs. (1)–(4)], which should not be valid far from T_c. This is the reason why we stop our calculations at temperatures below $T_c/3$. Therefore, at very low temperatures we do not know how to estimate the contributions of the islands with $T_c(i) \approx T_c$.

V. CONCLUSION

We have calculated the upper critical field $H_{c2}(T)$ for a disordered superconductor characterized by a distribution of different local critical temperatures $T_c(i)$ at different domains. We have applied a simple GL expression to each of these superconducting regions. With this procedure we can explain the magnetic signals below and above T_c. We have been able to fit the H_{c2} curves derived by two different experimental procedures, namely, the resistive magnetic fields and the Nernst signal.[30] In all the cases the curves exhibit a positive curvature which is different from the magnetically determined H_{c2} lines[41] from a pure GL approach [Eq. (3)]. This positive curvature reflects the GL behavior of each individual domain in a disordered superconductor. Furthermore, taking the inhomogenous charge distribution into account several properties like the Meissner and Nernst effects, which are seen at temperatures much higher than T_c, are naturally explained. Such inhomogeneities are taken into account by a charge distribution, but as discussed above, the main features of our calculations are independent of the details of the probability charge distribution. In conclusion, it is crucial to take into consideration the fact that HTSCs are inhomogeneous materials in order to describe the main qualitative features of the high-T_c superconductors.

[1] J.G. Bednorz and K.A. Müller, Z. Phys. **64**, 189 (1986).
[2] Y. Ando, G.S. Boebinger, A. Passner, L.F. Schneemeyer, T. Kimura, M. Okuya, S. Watauchi, J. Shimoyama, K. Kishio, K. Tamasaku, N. Ichikawa, and S. Uchida, Phys. Rev. B **60**, 12475 (1999).
[3] M.S. Osofsky, R.J. Soulen, Jr., S.A. Wolf, J.M. Broto, H. Rakoto, J.C. Ousset, G. Coffe, S. Askenazy, P. Pari, I. Bozovic, J.N. Eckstein, and G.F. Virshup, Phys. Rev. Lett. **71**, 2315 (1993).
[4] A.P. Mackenzie, S.R. Julian, G.G. Lonzarich, A. Carrington, S.D. Hughes, R.S. Liu, and D.C. Sinclair, Phys. Rev. Lett. **71**, 1238 (1993).
[5] G. Kotliar and C.M. Varma, Phys. Rev. Lett. **77**, 2296 (1996).
[6] G. Blatter, M.V. Feigel'man, V.B. Geshkenbein, A.I. Larkin, and V.M. Vinokur, Rev. Mod. Phys. **66**, 1125 (1994).
[7] E. Helfand and N.R. Werthamer, Phys. Rev. Lett. **13**, 686 (1964).
[8] N.R. Werthamer, E. Helfand, and P.C. Hohenberg, Phys. Rev. **147**, 295 (1966).
[9] G. Kotliar and A. Kapitulnik, Phys. Rev. B **33**, 3146 (1986).
[10] Yu.N. Ovchinnikov and V.Z. Kresin, Phys. Rev. B **52**, 3075 (1995).
[11] B. Spivak and F. Zhou, Phys. Rev. Lett. **74**, 2800 (1995).
[12] V.B. Geshkenbein, L.B. Ioffe, and A.J. Millis, Phys. Rev. Lett. **80**, 5778 (1998).
[13] T. Domanski, M.M. Maśka, and M. Mierzejewski, Phys. Rev. B **67**, 134507 (2003).
[14] A.J. Schofield, Phys. Rev. B **51**, 11733 (1995).
[15] R.G. Dias and J.M. Wheatley, Phys. Rev. B **50**, 13887 (1994).
[16] A.S. Alexandrov, Phys. Rev. B **48**, 10571 (1993).
[17] M. Mierzejewski and M.M. Maśka, Phys. Rev. B **66**, 214527 (2002).
[18] S.H. Pan, J.P. O'Neal, R.L. Badzey, C. Chamon, H. Ding, J.R. Engelbrecht, Z. Wang, H. Eisaki, S. Uchida, A.K. Gupta, K.W. Hudson, K.M. Lang, and J.C. Davis, Nature (London) **413**, 282 (2001); cond-mat/0107347 (unpublished).
[19] K.M. Lang, V. Madhavan, J.E. Hoffman, E.W. Hudson, H. Eisaki, S. Uchida, and J.C. Davis, Nature (London) **415**, 412 (2002).
[20] C. Howald, P. Fournier, and A. Kapitulnik, Phys. Rev. B **64**, 100504 (2001).
[21] T. Egami and S.J.L. Billinge, in *Physical Properties of High Temperature Superconductors V*, edited by D.M. Ginzberg (World Scientific, Singapore, 1996) p. 265.
[22] S.J.L. Billinge, E.S. Bozin, and M. Gutmann, cond-mat/0005032 (unpublished).
[23] E.S. Bozin, G.H. Kwei, H. Takagi, and S.J.L. Billinge, Phys. Lett. B **84**, 5856 (2000).
[24] T. Egami, Proc. of the New 3SC International Conference,

Physica C **364-365**, 561 (2001), and references therein.
[25] E.V.L. de Mello, M.T.D. Orlando, J.L. González, E.S. Caixeiro, and E. Baggio-Saitovich, Phys. Rev. B **66**, 092504 (2002).
[26] E.V.L. de Mello, E.S. Caixeiro, and J.L. González, Phys. Rev. B **67**, 024502 (2003).
[27] T. Timusk and B. Statt, Rep. Prog. Phys. **62**, 61 (1999).
[28] I. Iguchi, I. Yamaguchi, and A. Sugimoto, Nature (London) **412**, 420 (2001).
[29] A. Lascialfari, A. Rigamonti, L. Romano, P. Tedesco, A. Varlamov, and D. Embriaco, Phys. Rev. B **65**, 144523 (2002).
[30] Y. Wang, Z.A. Xu, T. Kakeshita, S. Uchida, S. Ono, Y. Ando, and N.P. Ong, Phys. Rev. B **64**, 224519 (2001).
[31] Y. Wang, N.P. Ong, Z.A. Xu, T. Kakeshita, S. Uchida, D.A. Bonn, and W.N. Hardy, Phys. Rev. Lett. **88**, 257003 (2002).
[32] J.M. Trancada, B.J. Sternlieb, J.D. Axe, Y. Nakamura, and S. Uchida, Nature (London) **375**, 561 (1995).
[33] A. Bianconi, N.L. Saini, A. Lanzara, M. Missori, T. Rossetti, H. Oyanagi, H. Yamaguchi, K. Oka, and T. Ito, Phys. Rev. Lett. **76**, 3412 (1996).
[34] Z.A. Xu, N.P. Ong, Y. Wang, T. Kakeshita, and S. Ushida, Nature (London) **406**, 486 (2000).
[35] M. Oda, N. Momono, and M. Ido, Supercond. Sci. Technol. **13**, R139 (2000).
[36] D.S. Fisher, M.P.A. Fisher, and D.A. Huse, Phys. Rev. B **43**, 130 (1991).
[37] L.N. Bulaevskii, Int. J. Mod. Phys. B **4**, 1849 (1990).
[38] W.E. Lawrence and S. Doniach, in *Proc. of the 12th Int. Conf. of Low-Temperature Physics*, Kyoto, 1970, edited by E. Kanda (Keigaku, 1970), p. 361.
[39] M. Cyrot and D. Pavuna, *Introduction to Superconductivity and High-T_c Materials* (World Scientific, Singapore, 1992).
[40] M. Franz, C. Kallin, A.J. Berlinsky, and M.I. Salkola, Phys. Rev. B **56**, 7882 (1997).
[41] Q. Li, M. Suenaga, T. Kimura, and K. Kishio, Phys. Rev. B **47**, 11384 (1993).
[42] I.L. Landau and H.R. Ott, Phys. Rev. B **66**, 144506 (2002).
[43] I.L. Landau and H.R. Ott, Physica C **385**, 544 (2003).
[44] V.L. Ginzburg, Zh. Éksp. Teor. Fiz. **23**, 236 (1952).
[45] Y.J. Uemura, Solid State Commun. **126**, 23 (2003).
[46] S.L. Cooper and K.E. Gray, in *Physical Properties of High Temperature Superconductors IV*, edited by Donald M. Ginsberg (World Scientific, Singapore, 1994), p. 122.